Free Energy Calculations of Conformational Equilibrium of Chorismate in Water. The Role of Solute Polarization

Sergio Madurga and Eudald Vilaseca*

Departament de Química Física i Centre de Recerca en Química Teòrica, Facultat de Química, Universitat de Barcelona, Martí i Franquès 1, 08028-Barcelona, Catalunya, Spain

Received: July 9, 2002; In Final Form: September 30, 2002

The conformational equilibrium of chorismate molecule in water has been studied with Monte Carlo free energy perturbation simulations. Relative solvation free energies of chorismate conformations have been calculated using three types of perturbation paths depending on the intermolecular solute−solvent energy terms considered. First, smooth transformation between solute conformations are performed without consideration of chorismate site charges. Second, the solvation free energy contribution because of the inclusion of electrostatic solute−solvent interactions are calculated. Finally, the role of polarization forces are studied introducing progressively atom polarizabilities in the chorismate molecule. The calculation of relative free energies through these three perturbation paths allows the comparison of the different energetic forces, and improves the convergence of the results. It has been found that the inclusion of solute polarization is crucial to obtain diequatorial−diaxial conformational proportions compatible with the experimental values. Different procedures to calculate solute polarization are analyzed depending on the way the intramolecular interactions among the polarization sites of chorismate are treated. Two types of water models, polarizable and nonpolarizable, have been considered. A hydrogen bond analysis and a study of the role of the charge variations among chorismate conformations are also done.

1. Introduction

Chorismate molecule (Scheme 1) is a precursor of aromatic amino acids and other metabolites in bacteria, fungi, and plants.[1,2] Its intramolecular Claisen rearrangement can be observed at the active site of the enzyme chorismate mutase and also in aqueous solution.[3,4] This reaction has attracted theoretical interest because it is an unusual case of enzyme-catalyzed pericyclic reaction where the catalytic enzyme activity is done without forming a chemical bond with the substrate.[5−11] A better understanding of the aqueous and enzymatic reactivity of chorismate can be obtained with a complete knowledge of the conformational variability of this molecule in solution.

The conformations of chorismate dianion can be classified into two groups, pseudodiequatorial and pseudodiaxial, depending on the position of the ether and the hydroxy oxygen atoms with respect to the cyclohexadienyl ring (hereafter, they will be distinguished as diequatorial and diaxial).

Conformational studies of chorismate in water have been performed by both, discrete and continuum solvent techniques. Hillier et al.[12] studied the effect of solvation by means of a polarizable continuum model (PCM). These calculations yielded a greater population for the diequatorial conformation than what it was expected from the experimental ^{1}H NMR data.[4] In a recent study,[13] diequatorial−diaxial conformational proportions compatible with the experimental values were obtained using a polarizable continuum model (PCM) with a cavity definition of the united atom model for Hartree−Fock (UAHF).

Conformational studies of chorismate in water by means of free energy perturbation (FEP) simulations were first performed by Carlson and Jorgensen.[14] They obtained a diequatorial-diaxial free energy difference of 3.6 kcal/mol, three times greater than the experimental value. Hillier et al.[12] performed new FEP simulations for the conformational equilibrium considering an additional diaxial minimum. They obtained similar results to those of Carlson and Jorgensen.[14]

SCHEME 1

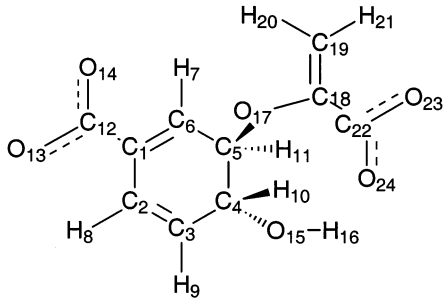

In the present work, the description of the conformational equilibrium of chorismate with FEP simulations is improved in two ways: by incorporating new minima found in gas phase and in solution[13] and by the inclusion of a polarization potential in the system force field. Several procedures have been employed to calculate the solute polarization. The role of the polarization of solvent molecules is also studied.

2. Computational Details

FEP calculations were carried out with a Monte Carlo simulation program of our group in the isothermal−isobaric (NPT) ensemble at 25 °C and 1 atm. All studied systems consist of one molecule of chorismate in a rigid conformation and 1400 molecules of water. System configurations were generated by selecting a molecule at random and changing, also randomly,

* To whom correspondence should be addressed. Fax: 34−93 4021231. E-mail: eudald@qf.ub.es.

10.1021/jp026482d CCC: $22.00
Published on Web 11/12/2002

SCHEME 2

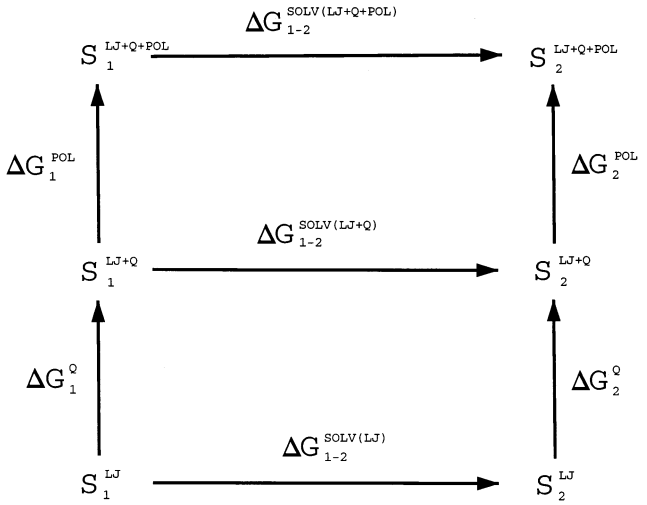

its coordinates. The ranges for translational, rotational motions, and attempted volume changes were adjusted to yield an approximate acceptance rate of 40%. As the main interest of the simulations is focused on solute properties, the preferential sampling algorithm was used. The weighting function to choose water molecules to attempt a movement is similar to that of a previous work[15]

$$w(r_{\min}) = 1/(r_{\min}{}^2 + cte) \tag{1}$$

where *cte* is a constant with 120 Å^2 value and $r_{\min}$ is defined as the distance between the oxygen atom of a water molecule and its nearest oxygen atom of the chorismate molecule. To obtain a correct implementation of this sampling procedure, the acceptance probability in the Metropolis test was modified as usual.[16−18]

Free energy perturbations were performed with the Zwanzing's perturbation expression

$$\Delta G_{0\rightarrow 1} = -k_B T \ln \langle \exp(-\Delta H/k_B T)\rangle_0 \tag{2}$$

The average refers to sampling configurations for the reference state 0, k_B is the Boltzmann constant, T is the temperature, and ΔH is calculated as the difference between the total potential energies of states 0 and 1. To construct the FEP paths, it is convenient to define a coupling parameter λ that allows the smooth conversion of system 0 to 1. Then, the progressive mutation of any geometrical or potential parameter (ζ) can be expressed as

$$\zeta(\lambda) = \zeta_0 + \lambda(\zeta_1 - \zeta_0) \tag{3}$$

where λ goes from 0 to 1 through a certain number of steps (windows). The total free energy is calculated as the sum of the individual free energy changes of all windows. Each individual free energy is the average of the forward and backward change values. At the same time, the difference between the forward and backward change values (hysteresis) is used to estimate the statistical errors.

The conformational structures of chorismate molecule were taken from a previous work[13] where a conformational analysis in the gas phase and in a continuum model solvent was done. In that study, the gas phase conformational minima of chorismate were obtained from optimizations at the HF/6-31G* level and their energies were computed at the MP2/6-31+G* level.

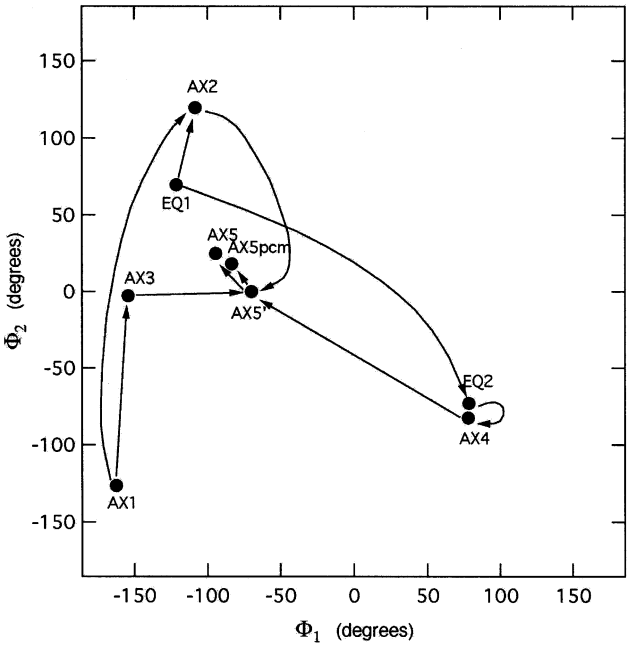

Figure 1. Schematic representation of LJ transformations between conformations. Chorismate conformations are situated as a function of ϕ_1 ($C_6 - C_5 - O_{17} - C_{18}$) and ϕ_2 ($C_5 - O_{17} - C_{18} - C_{19}$) torsional angles of the main side chain.

Relative solvation free energies of chorismate conformations have been calculated through a decomposition in several steps (Scheme 2). In a first step, the relative free energy of solvation with a simple modeling of the solute is computed ($\Delta G^{\mathrm{SOLV(LJ)}}$). Transformations among conformations are performed with FEP simulations using only Lennard-Jones (LJ) sites in the chorismate molecule. At this stage, the free energies yield an unreal equilibrium because the chorismate dianion is treated as a hydrophobic molecule. However, the transformations among chorismate conformations calculated in this way yield more converged results than if they were obtained using both, LJ and charge sites. The second step is the inclusion of the electrostatic contribution for each individual conformation (ΔG^{Q}). It could be obtained from FEP simulations of a charge process for each conformation. However, these simulations have been performed in the reverse sense, the discharge process. Thus, the sign of the discharge free energy should be changed to be added to the rest of the free energy contributions. In the last step, the contribution of the polarization to the free energy of solvation has been computed by introducing the polarization sites through FEP simulations (ΔG^{POL}). As the free energies of these three processes are well separated, the contributions of the Lennard-Jones, electrostatic, and polarization free energies to the global equilibrium can be analyzed.

As a result, three types of perturbation paths were defined to calculate the free energies of the previous processes: (1) LJ transformations between conformations. Chorismate conformations have been connected according to Figure 1. All of the conversions were performed with 20 windows, except for the AX5′ → AX5 and AX5′ → AX5pcm transformations which required only 7 and 5 windows, respectively. A total of 7×10^6 configurations of equilibration between windows and 16×10^6 configurations of averaging in each windows were done. (2) Discharge process. The electrostatic contribution for each conformation was calculated decreasing linearly the formal charges of solute atoms to 0 through 160 windows. Each window consists of 1×10^6 configurations of equilibration and 5×10^6 configurations of averaging. (3) Polarization process.

The contribution of the polarization energy of each conformation was calculated introducing linearly the atomic polarizability of each solute atom through 20 windows. Each window consists of 1×10^6 configurations of equilibration and 2×10^6 configurations of averaging.

Two types of water models were employed: the nonpolarizable TIP4P water model[19] and the polarizable DC water model.[20] The geometrical parameters of the two types of water are identical, but they differ in the LJ parameter and charge values. In addition, the DC water model includes a point polarizability ($\alpha = 1.44$ Å^3) on the bisector of the H−O−H angle at 0.215 Å away from the oxygen atom.

The intermolecular interaction energy of the system for the most complete case is calculated as

$$U = U^{\mathrm{PAIR}} + U^{\mathrm{POL}} \tag{4}$$

The U^{PAIR} pairwise additive energetic term has two contributions

$$U^{\mathrm{PAIR}} = U^{\mathrm{LJ}} + U^{\mathrm{qq}} \tag{5}$$

The Lennard-Jones interaction energy is calculated as

$$U^{\mathrm{LJ}} = \sum_{i,j>i}^{N} \sum_{A,B\neq A}^{N_{\mathrm{SLJ}}} 4\epsilon_{A,B}\left[\left(\frac{\sigma_{A,B}}{r_{iA,jB}}\right)^{12} - \left(\frac{\sigma_{A,B}}{r_{iA,jB}}\right)^{6}\right] + U_{\mathrm{LJ}}^{\mathrm{corr}} \tag{6}$$

where N is the total number of molecules of the system and N_{SLJ} is the number of LJ sites in the solute or in the solvent molecules. The $r_{iA,jB}$ is the distance of site A in molecule i from site B in molecule j. Lennard-Jones parameters for chorismate molecule are OPLS all-atom values taken from literature.[21−23] The usual combining rules were used to calculate ϵ and σ values for chorismate-water interactions. The long-range correction for the Lennard-Jones interactions, $U_{\mathrm{LJ}}^{\mathrm{corr}}$, is calculated assuming that the partial pair-correlation functions are the unity beyond the cutoff R_c

$$U_{\mathrm{LJ}}^{\mathrm{corr}} = \frac{8\pi}{3}\frac{N_c\rho_m}{{R_c}^3}\epsilon\sigma^6\left[\frac{1}{3}\left(\frac{\sigma}{R_c}\right)^6 - 1\right] \tag{7}$$

being ρ_m the number density of molecules, and N_c the number of molecules with the same (σ,ϵ) values.

U^{qq} term in eq 5 is the energy of the system because of charge−charge interactions corrected with the reaction field method:

$$U^{\mathrm{qq}} = \frac{1}{4\pi\epsilon_0}\left[\frac{c_{\mathrm{RF}}}{2}N_{\mathrm{H_2O}}\vec{m}_i^{\,2} + \sum_{i,j>i}^{N}\sum_{A,B\neq A}^{N_{\mathrm{Sq}}}\frac{q_A q_B}{r_{iA,jB}}\left(1 + \frac{c_{\mathrm{RF}}}{2}{r_{iA,jB}}^3\right)\right] \tag{8}$$

where $N_{\mathrm{H_2O}}$ is the number of water molecules and N_{Sq} is the number of electrostatic sites in the solute or in the solvent molecules. The formal charges of the electrostatic sites of chorismate, q, have been obtained with the CHELPG method[24] implemented in Gaussian package[25] from the HF/6-31+G* gas-phase wave function for each conformation. The c_{RF} is the reaction field correction factor, ϵ_0 is the vacuum permittivity, and $\vec{m}_i$ is the permanent dipole moment of water molecules.

The polarization term in eq 4 is calculated as

$$U^{\mathrm{POL}} = -\frac{1}{2}\sum_{i=1}^{N}\sum_{A}^{N_P}\vec{\mu}_{iA}^{\mathrm{ind}}\vec{E}_{iA}^{\mathrm{q}} \tag{9}$$

where N_P is the number of polarization sites of each molecule i (1 for water and 24 for chorismate). The $\vec{\mu}_{iA}^{\mathrm{ind}}$ induced dipole moments can be expressed as

$$\vec{\mu}_{iA}^{\mathrm{ind}} = \alpha_{iA}(\vec{E}_{iA}^{\mathrm{q}} + \vec{E}_{iA}^{\mathrm{d}}) \tag{10}$$

where α_{iA} is the polarizability of site A in molecule i, $\vec{E}_{iA}^{\mathrm{q}}$ and $\vec{E}_{iA}^{\mathrm{d}}$ are the electric fields at the position of $\vec{\mu}_{iA}^{\mathrm{ind}}$ because of the fixed charges of the electrostatic sites and to the induced dipole moments of the other polarization sites, respectively. A single-point polarizability was defined for the DC solvent molecules,[20] whereas point polarizabilities were introduced in all atoms of chorismate molecule to account for the nonadditive induced polarization effect. The atomic site polarizabilities were taken from the interaction model of Applequist et al.[26,27]

The electric fields produced by the permanent charges and by the induced dipole moments can be calculated as

$$\vec{E}_{iA}^{\mathrm{q}} = \frac{1}{4\pi\epsilon_0}\left[c_{\mathrm{RF}}\vec{m}_i + \sum_{j}^{N}\sum_{B\neq A}^{N_{\mathrm{Sq}}}\frac{q_B}{{r_{iA,jB}}^3}\vec{r}_{iA,jB}(1 - c_{\mathrm{RF}}{r_{iA,jB}}^3)\right] \tag{11}$$

and

$$\vec{E}_{iA}^{\mathrm{d}} = \frac{1}{4\pi\epsilon_0}\left[c_{\mathrm{RF}}\vec{\mu}_{iA}^{\mathrm{ind}} + \sum_{j}^{N}\sum_{B\neq A}^{N_P}\frac{1}{r_{iA,jB}^3}\left[\frac{3\vec{r}_{iA,jB}\vec{\mu}_{jB}^{\mathrm{ind}}}{{r_{iA,jB}}^2}\vec{r}_{iA,jB} - \vec{\mu}_{jB}^{\mathrm{ind}}(1 - c_{\mathrm{RF}}{r_{iA,jB}}^3)\right]\right] \tag{12}$$

The reaction field correction factor, c_{RF}, can be written as

$$c_{\mathrm{RF}} = \frac{2(\epsilon_{\mathrm{RF}} - 1)}{2\epsilon_{\mathrm{RF}} + 1}\frac{1}{{R_c}^3} \tag{13}$$

where R_c is the interaction cutoff distance and ϵ_{RF} is the dielectric constant of the continuum beyond R_c. In the solvent−solvent interactions, the R_c cutoff distance was based on the oxygen−oxygen distances. For Lennard-Jones and electrostatic terms, the cutoff is set at 8.5 Å, whereas for polarization terms, the cutoff is reduced to 7.0 Å. Solute−solvent interactions were set to zero when the distance between the water oxygen and its nearest chorismate oxygen is greater than 12.5 Å for Lennard-Jones and electrostatic terms and 11.0 Å for polarization terms. The reduction in the polarization cutoff is needed to accelerate the calculation of the polarization energy of the system. This reduction can be done because of the faster decay of the polarization interactions. The polarization energy of the system at every configuration was calculated using eqs 10−12 in an iterative procedure, because the induced dipole moment of each polarization site depends on the induced dipole moments of the other polarization sites. The iterative process was stopped when the variation of the polarization energy between two consecutive cycles was smaller than 0.01 kcal/mol. A more precise criterion, 0.001 kcal/mol, was applied to the system configurations selected for the calculation of the average free energy differences.

3. Results and Discussion

3.1. LJ Transformations between Conformations. In the first type of perturbation paths, only LJ interaction sites are defined in the solute. Although van der Waals energy terms are only used to describe water−chorismate interactions, water−

TABLE 1: Free Energy Change for the LJ Transformations between Chorismate Conformations in Water[a]

conversion	ΔG	hysteresis	number of calcs	stdev (disp)	stdev (blocks)
AX1 → AX2	−0.48	0.29	4	0.53	0.14
AX1 → AX3	−0.33	0.63	4	0.99	0.19
AX3 → AX5′	0.19	0.31	4	0.26	0.12
AX2 → AX5′	−0.64	0.30	4	0.57	0.15
AX4 → AX5′	0.07	0.18	2		0.16
EQ1 → AX2	0.80	0.19	2		0.15
EQ1 → EQ2	−0.34	0.05	2		0.11
EQ2 → AX4	0.44	0.06	2		0.11
AX5′ → AX5	0.37	0.03	1		0.04
AX5′ → AX5pcm	0.04	0.07	1		0.05

[a] Hysteresis values are the average values of several FEP calculations. stdev(disp) are calculated from the dispersion of the different free energy values obtained for each conversion. stdev(blocks) are the accumulated stdev values calculated using the batch means procedure for each window. All energetic values are in kcal/mol.

TABLE 2: Relative Gas Phase Energies and Contributions to the Relative Solvation Free Energy of the Chorismate Molecule Conformations (Energies in kcal/mol)

conformation	ΔE^{GAS}	$\Delta G^{SOLV(LJ)}$	ΔG^{Q}	ΔG^{POL}_{DC}	ΔG^{POL1}_{TIP4P}	ΔG^{POL2}_{TIP4P}	ΔG^{POL3}_{TIP4P}
EQ1	0	0.3	7.9	−8.7	−8.0	−9.1	−8.9
EQ2	1.9	0	7.0	−7.7	−7.6	−9.5	−9.0
AX1	10.1	1.6	4.2	−6.4	−6.1	−11.4	−10.1
AX2	10.6	1.1	5.5	−5.4	−6.0	−9.7	−9.3
AX3	11.7	0.3	0.0	−4.8	−5.5	−12.3	−11.1
AX4	14.8	0.4	3.2	−5.6	−5.9	−9.4	−8.7
AX5	11.0	0.9	1.0	−6.3	−5.9	−11.2	−10.6
AX5pcm	11.7	0.6	2.4	−6.1	−5.8	−11.4	−10.1

water interactions are described using the LJ site centered in the oxygen and also the three charge sites of the TIP4P water model. This type of simulations consist of transforming one conformation of chorismate into another progressively through 20 windows. The path of transformation has been constructed linearly varying the bond distances, angles, and torsions from the initial state to the final state. Free energies have been calculated using the Zwanzig's expression (eq 2) for the perturbations to the forward and backward structure. In each window, the perturbed solute structure is located in a position that minimizes the root-mean-square displacement of all atoms with respect to the unperturbed structure.

Table 1 shows the change in free energy for several conversions between nine conformational structures of chorismate. Seven of them (AX1, AX2, AX3, AX4, AX5, EQ1, and EQ2) are gas-phase minima, the AX5pcm conformation corresponds to a PCM minimum found in solution in a previous work,[13] and the AX5′ structure corresponds to a partial gas phase optimization employed to connect several minima.

Small free energies, less than 1 kcal/mol, are needed to perform each conversion (Table 1), which is a consequence of the weak solute−solvent LJ interactions. Second column of Table 2 shows the relative LJ free energies of solvation for each conformation ($\Delta G^{SOLV(LJ)}$) indicating that the most stabilized structure is the EQ2 minimum and that the general trend is to produce a greater stabilization of the two diequatorial conformations. As the LJ parameters of the chorismate sites have always the same values for all of the studied conformations, the free energy changes should reflect differences in conformational shapes. To see this effect, the molecular volume was calculated for each conformation (Table 3). This volume is defined as the volume contained by the surface of van der Waals contact between the chorismate conformation and a water molecule. It can be seen that the conformations with smaller molecular volume (EQ1, EQ2, and AX4) are well stabilized by LJ interactions (relative free energies of 0−0.4 kcal/mol). Conformations with greater volumes (AX1, AX2, AX5, and AX5pcm) have higher relative free energies (0.6−1.6 kcal/mol). The AX3 conformation with a high volume and a low relative free energy is the exception. However, the general trend is in good agreement with the hydrophobic effect, which is favored by the no inclusion of the electrostatic contribution in the chorismate sites. In Table 3, the distance between the two reactive carbon atoms in the intramolecular Claisen rearrangement of chorismate is also shown. Among the diaxial conformations, the AX4 structure is the only one near the transition state. In addition, the diequatorial EQ2 conformation, having also a short intramolecular reactive carbon−carbon distance, can be relevant as a starting point of the reaction path. As a consequence of their greater proximity to the cyclic transition state, their molecular volumes are also the smallest of all studied conformations.

TABLE 3: Molecular Volumes and C1−C19 Distances for the Chorismate Conformations[a]

conformation	volume	d(C1−C19)
EQ1	688.8	5.07
EQ2	678.9	4.38
AX1	694.2	5.33
AX2	694.3	4.91
AX3	694.8	5.31
AX4	680.2	3.78
AX5	697.9	4.70
AX5pcm	696.5	4.54
AX5′	696.5	4.45

[a] Volumes are in Å^3, and distances are in Å.

A first error analysis for these conformational conversions was done with the resulting hysteresis of the free energy perturbations. The first four conversions shown in Table 1 were repeated four times because their hysteresis values are greater than those of the other conversions. Additionally, it is possible to obtain an estimation of the standard deviation (stdev) of the four free energy values of each of these four conversions and compare it with the hysteresis values obtained through the simulations. As can be seen, the conversion with the highest stdev has also the highest mean hysteresis. However, in three of the four cases, hysteresis indicates less error than stdev. The next four conversions, with a hysteresis smaller or equal than 0.2 kcal/mol, were repeated two times. Finally, the short connections between the AX5′ and the AX5 minimum and the AX5′ and the AX5pcm structure were computed only one time because of their small hysteresis and the small conformational change involved, 7 and 5 windows, respectively.

Another method to obtain the stdev of a conversion consists of the accumulation of the stdev of all of the windows computed with the batch means procedure. Last column in Table 1 shows the stdev values obtained for all of the conversions when the batch means procedure is done with 20 blocks for each window. It can be seen that the method of blocks always yields less error than the stdev calculated through independent repetitions and also is smaller than the mean values of the hysteresis. Calculations of the stdev with a different number of blocks have been performed but no significant change was observed. A convergence study of the stdev with the batch means procedure was performed for three separated windows of the AX1 → AX3 conversion with a large number of configurations (192M). The results indicate that more than 50M of configurations for window are needed to obtain an uncorrelated stdev using the batch means procedure. This slow convergence in the stabilization of the stdev indicates the slow convergence of the free energy calculations when the rotation of dihedral angles of chorismate is performed.

TABLE 4: RMSD for Conversions between Chorismate Conformations[a]

conversion	RMSD (all)	RMSD (1−15)	RMSD (17−24)	RMSD (20&24)
AX1 → AX2	0.061	0.037	0.092	0.143
AX1 → AX3	0.078	0.043	0.120	0.186
AX3 → AX5′	0.058	0.040	0.083	0.111
AX2 → AX5′	0.057	0.030	0.089	0.131
AX4 → AX5′	0.077	0.063	0.099	0.097
EQ1 → AX2	0.079	0.075	0.060	0.074
EQ1 → EQ2	0.055	0.047	0.070	0.056
EQ2 → AX4	0.064	0.058	0.039	0.052
AX5′ → AX5	0.033	0.029	0.040	0.038
AX5′ → AX5pcm	0.029	0.022	0.039	0.046

[a] Each column shows the average RMSD for the group of atoms indicated in parenthesis. See Scheme 1 for atom numbering. RMSD units are in Å.

As a result, a part from the AX1 → AX3 conversion, the error for the LJ conversions can be estimated about 0.3 kcal/mol. This value is obtained from the stdev of the conversions repeated four times, which are the conversions with the greatest error. The other conversions, with smaller hysteresis, can be expected to have smaller error.

Table 4 shows the root-mean-square displacement (RMSD) for several groups of atoms of chorismate averaged over all of the windows of each conformational conversion. It can be seen that the conversions performed with 20 windows show similar values for the RMSD of the group of all solute atoms. They fall in the range of 0.06−0.08 Å. No correlation between these values and the error estimation of the free energy of the conformational conversions (Table 1) is observed. The calculated RMSD for the 1−15 atom group of chorismate (ring section) and for the 17−24 atom group (main side chain) are also shown in Table 4. See Scheme 1 for atom numeration. The hydrogen of the hydroxyl group, atom no. 16, is not considered because it is the only atom that has not LJ parameters. Because the major change among minima comes from the disposition of the main side chain, the RMSD of the 17−24 atom group presents greater differences among conversions than the observed for the ring section. On the other hand, a good correlation between the hysteresis and the calculated errors for the free energy of the conformational conversions is obtained when the RMSD is calculated for the atoms nos. 20 and 24 (Scheme 1). These two atoms, because of their position, are the most sensitive to the movement of the main side chain and are the worst fitted in the construction of the conversion paths. This good correlation indicates that free energy errors of the LJ conversions are mainly determined by the worst fitted atoms.

With the conversions of Table 1, it is possible to establish two thermodynamic cycles. The free energy of one cycle can be calculated with the free energy of four conversions: ΔG(AX1 → AX2) − ΔG(AX1 → AX3) − ΔG(AX3 → AX5′) + ΔG(AX2 → AX5′), and it closes with −0.98 kcal/mol. The other cycle is calculated using five conversions: − ΔG(AX2 → AX5′) + ΔG(AX4 → AX5′) − ΔG(EQ1 → AX2) + ΔG(EQ1 → EQ2) + ΔG(EQ2 → AX4) yielding a closure energy of 0.01 kcal/mol. This excellent closure is clearly fortuitous as can be inferred from the obtained hystereses, whereas the obtained closure energy for the first cycle is compatible with the accumulation of the estimated errors in each conversion.

Because of the construction of thermodynamic cycles the connection between every two structures can be performed through two paths. Relative LJ free energies of solvation of Table 2 have been calculated without the consideration of the AX1 → AX3 conversion because of its biggest error. As the errors of the mean values of free energies for the other conversions are estimated to be similar or less than 0.3 kcal/mol, a maximum error of 0.3 kcal/mol can be assigned to each $\Delta G^{SOLV(LJ)}$ free energy value.

3.2. Discharge Process. Free energy discharge calculations were performed for each conformation through many steps, 160 windows, because of the high electrostatic solvation energy of the chorismate dianion. For example, the AX3 conformation has a variation of free energy for the discharge process of 234.2 kcal/mol. As can be expected for a dianion molecule, the free energy change for the charging process is very favorable for all chorismate conformations. Table 2 shows the relative values (ΔG^{Q}) obtained for the charging process of all conformations of the chorismate molecule. These relative values indicate that the diequatorial conformations are the less stabilized structures, whereas the most stabilized conformation is the AX3 minimum. Adding the first three columns of Table 2 —relative gas-phase energies, relative conformational LJ free energies, and relative electrostatic free energies— the relative global free energy of the chorismate conformations is obtained. From these values, it can be seen that the conformational equilibrium is totally moved to the diequatorial conformations, 63% for EQ1, 37% for EQ2, and only 0.1% for the diaxial conformations. Thus, although the electrostatic contribution favors the stabilization of the diaxial conformations, it is not sufficient to obtain conformational populations near the experimental values, 8−17% for the diaxial conformations.

The mean hysteresis obtained for these discharge free energy perturbations is 0.5 kcal/mol, whereas the stdev calculated with the batch means procedure is only 0.11 kcal/mol. Thus, as in the case of LJ simulations, the stdev obtained with the batch mean procedure is probably subestimating the correct value. Two different free energy discharge simulations have been performed for the EQ1, AX2, and AX3 conformations. From the differences between the two obtained free energy values, the error for the ΔG^{Q} values is estimated about 0.4 kcal/mol.

3.2.1. Hydrogen Bond Analysis. For each conformation, a Monte Carlo simulation of the chorismate−water solution was performed with LJ and electrostatic sites on the chorismate molecule to carry out a hydrogen bond analysis. The same TIP4P model was used for water molecules. Average values were obtained over 30×10^6 configurations, except for the simulation of the AX2 conformation which lasted 90×10^6 configurations. A geometric criterion of the H bond is used with three conditions. A hydrogen bond is formed when the distance between the oxygens of two molecules is less than 3.5 Å, the distance between the hydrogen and the oxygen of the H-bond acceptor is less than 2.5 Å, and the angle between the OH intramolecular bond of the H-bond donor and the line connecting the oxygens is less than 30 degrees. In Figure 2, the mean number of acceptor hydrogen bonds for each chorismate oxygen and the mean number of donor hydrogen bonds for the hydrogen of its hydroxyl group are shown for all minima structures. When the chorismate molecule adopts a diequatorial conformation, one H bond in one oxygen of the carboxylate group of the main side chain is lost because this oxygen is now immersed in an intramolecular hydrogen bond with the hydrogen of the hydroxyl group. It can be seen that, in EQ1 and EQ2 conformations, this hydrogen has no participation in any intermolecular hydrogen bond. The total number of hydrogen bonds between chorismate and water molecules are also shown in Figure 2. These values are in a range of 14.3−16.2 hydrogen bonds for all conformations. As can be expected, the diequatorial conformations have

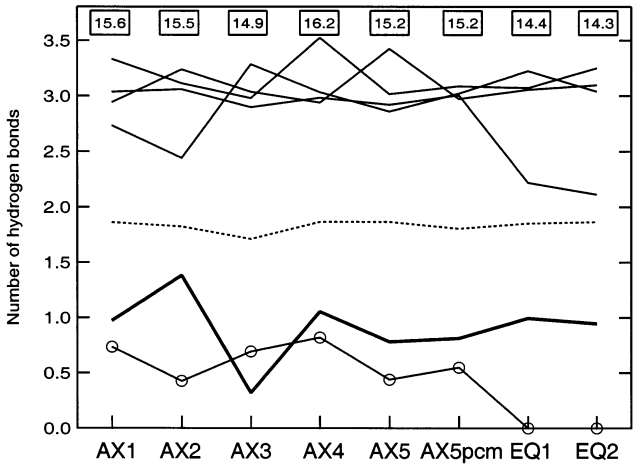

Figure 2. Number of hydrogen bonds between chorismate and water molecules for several selected atoms: carboxylate oxygens (thin line), ether oxygen (dashed line), hydroxyl oxygen (thick line), and hydroxyl hydrogen (line with circles). The total number of hydrogen bonds for each conformation is also displayed in boxes.

the smallest number of total hydrogen bonds. However, for the diaxial conformations, no correlation between the hydrogen bond number and the electrostatic stabilization is found. Thus, it is necessary to take into account more effects to explain the electrostatic stabilization. There can be important energetic differences among H bonds and also water molecules no H-bonded to the solute can have significant importance.

On the other hand, the number of water molecules with two simultaneous double bonds with the chorismate has also been computed. For each conformation, there is a probability of 5−10% to have a water molecule with a double bond with the two oxygens of the carboxylate groups. The AX2 conformation has an additional ∼25% probability of having a water H-bonded to the oxygen of the hydroxyl group and to one oxygen of the carboxylate group of the side chain. In previous studies,[14] it was thought that this water molecule H-bonded simultaneously to the carboxylate and hydroxyl oxygens is relevant in the stabilization of this conformation and in the description of the conformational equilibrium. However, as can be seen in the relative ΔG^{Q} values of the diaxial conformations (Table 2), the AX2 structure is the less stabilized, indicating that this additional water molecule does not affect significantly to the chorismate equilibrium.

3.2.2. CHELPG Charge Analysis. CHELPG charges of the chorismate atoms have been compared among all conformations. The charge of several atoms remains quite constant from one conformation to another. However, the ring sp3 C atoms and their hydrogens, the hydroxyl group, and the atoms of the double bond of the side chain have a variation range of their charge of $\sim 0.3e^{-}$.

To know the determinant factors for the relative solvation free energy ($\Delta G^{LJ} + \Delta G^{Q}$) of chorismate conformations, new free energy perturbations were performed to analyze the importance of the geometrical structure (st) and the assigned charges (q). In the Schemes 3 and 4, the transformation between two conformations (diagonal path) is decomposed into two steps. The diagonal path values are calculated from LJ and electrostatic free energies of Table 2. The vertical paths indicate the new free energy perturbations which transform atom charges without perturbing the structures. The horizontal paths, transformation of the conformational structure without changing atom charges, are calculated using a thermodynamic cycle. As can be seen in Scheme 3, in the transformation of the AX3

SCHEME 3: AX3-AX2 Conformational Transformation (Free Energies in kcal/mol)

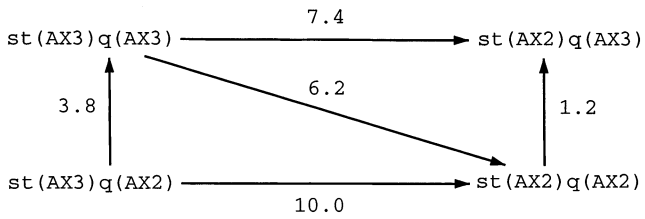

SCHEME 4: AX3-EQ1 Conformational Transformation (Free Energies in kcal/mol)

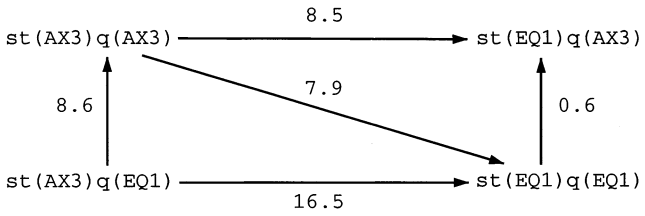

conformation (st(AX3)q(AX3)) to the AX2 conformation (st(AX2)q(AX2)), the transformations of the geometrical structure at fixed atom charges are more important than the corresponding vertical paths. In the transformation of AX3 conformation to EQ1 conformation (Scheme 4), a similar relation is obtained. However, free energies for the perturbations between AX3 and EQ1 charges are more important in the AX3 geometrical structure than in the EQ1 geometrical structure. Thus, although the relative stabilization of the conformations is mainly due to the change in the geometrical structure, the differences in the charge distribution are also very important, especially between the AX3 diaxial conformation and the EQ1 diequatorial conformation. Consequently, simulations of the conformational behavior of the chorismate molecule in water with the approximation of fixed charges would yield erroneous results.

3.3. Polarization Process. The variation of free energy produced by the inclusion of polarization sites on the chorismate molecule was calculated for each conformation. The polarization effect on the solute is described with atomic polarizabilities centered in each atom. The polarizability values are linearly scaled with free energy perturbations through 20 windows. Four types of polarization simulations were performed depending on the model of water employed (polarizable or nonpolarizable) and the way the intramolecular interactions among the polarization sites of chorismate are treated.

In the first case, the polarization of chorismate is studied with a DC polarizable water model. The polarization energy is a function of the electric fields created by the permanent charges of the system (solute and solvent molecules), E^{Q}, and by the induced dipole moments, E^{D}, on each polarization site (24 in chorismate and 1 in each water molecule). To avoid the polarization catastrophe (polarization energy becoming unrealistically large), the intramolecular 1−2 and 1−3 bonded interactions between charges and induced dipole moments of the solute are not considered in the calculation of E^{Q} and E^{D}.[28,29]

The absolute free energy of polarization obtained for each conformation with the DC model of water is shown in Table 2 (ΔG_{DC}^{POL} column). Each value is the free energy obtained in solution less the intramolecular free energy of polarization computed for the same chorismate conformation in gas phase. The stabilization caused by the free energy of polarization is greater in the diequatorial conformations than in the diaxial ones. This tendency yields conformational proportions more different

TABLE 5: Conformational Populations of Chorismate in DC Water Solution and in TIP4P Water Solution (POL1, POL2, and POL3 Models)[a]

conformation	% DC	% POL1	% POL2	% POL3	% expt
EQ1	94(8)	85(18)	49(31)	68(29)	88
EQ2	6(8)	15(18)	31(27)	27(27)	
AX1	0	0	0	0	
AX2	0	0	0	0	
AX3	0	0	19(19)	4.8(5.8)	12
AX4	0	0	0	0	
AX5	0	0	0.7(0.8)	0.5(0.6)	
AX5pcm	0	0	0	0	

[a] Proportion errors (in parentheses) are calculated considering a stdev of 0.6 kcal/mol for the total free energy of every conformation. The experimental populations for the diequatorial and the diaxial groups of conformations are also indicated[4].

from the experimental values (Table 5) than when only the LJ and electrostatic contributions are considered.

A second type of FEP simulations was performed with a nonpolarizable TIP4P water model. Three models (POL1, POL2, and POL3) have been studied depending on the intramolecular interactions of chorismate considered in the calculation of the polarization energy. As the TIP4P is a nonpolarizable solvent, in these three models, the polarization is only produced in the solute.

In the POL1 model, the polarization energy is calculated considering the TIP4P charges of the solvent molecules and the intramolecular chorismate interactions between charges and induced dipoles separated by three or more bonds. The polarization energy because of the intramolecular interactions between the polarization sites of chorismate in the gas phase is subtracted from the free energy in solution yielded by the simulations. The obtained free energy values, $\Delta G_{\mathrm{TIP4P}}^{\mathrm{POL1}}$, are shown in Table 2. It can be seen that the $\Delta G_{\mathrm{TIP4P}}^{\mathrm{POL1}}$ values are very similar to the previous $\Delta G_{\mathrm{DC}}^{\mathrm{POL}}$ free energies. Thus, the free energy variation of the process of including polarizability sites in the chorismate molecule seems to be independent from the fact that solvent molecules were explicitly polarizable or that they had the polarization included in an average way. With respect to the effect on each chorismate conformation, the free energy of polarization yields an increase of diequatorial proportions. As can be seen from the first two columns of Table 5, only the diequatorial conformations are significantly populated in these two models. As will be discussed in the POL2 model, proportion errors in Table 5 are obtained estimating an error of 0.6 kcal/mol for the total free energy of each conformation. The errors obtained for diequatorial conformations are large because little variations of free energy yield great changes in the proportions. According to these two models, the EQ1 structure is more populated than the EQ2 conformation.

In the POL2 model, the E^{Q} electric field on the polarization sites of the chorismate is calculated as a function of only the charges of the TIP4P waters. Charges on the chorismate sites do not affect directly to the polarization energy terms, but an iterative procedure is also needed because the inductive effect between induced dipole moments of the chorismate molecule situated at a distance of three or more bonds is considered. Free energy results for this model, $\Delta G_{\mathrm{TIP4P}}^{\mathrm{POL2}}$, are shown in Table 2. Each free energy value corresponds to the average of two FEP simulations. With this model, the diaxial conformations are more stabilized than the diequatorial ones. It can be seen that the most stabilized conformation, AX3, is also the most stabilized by the electrostatic interactions. This conformation is now about 3 kcal/mol more stable than the diequatorial conformations. Adding all free energy contributions (ΔE^{GAS}, ΔG^{LJ}, ΔG^{Q}, and $\Delta G_{\mathrm{TIP4P}}^{\mathrm{POL2}}$), the total free energy differences among conformations are obtained for this model, and from that, the relative proportions are calculated (Table 5). As can be seen, the conformational proportions are compatible with the experimental values. The AX3, with 19%, and the AX5, with 1%, minima are the two more populated diaxial conformations. In contrast with the previous models, the two diequatorial conformations are now similarly populated.

The errors in the conformational proportions are shown in parentheses in Table 5. These errors have been computed estimating an error of 0.6 kcal/mol for the total free energy of each conformation. This value has been obtained from the accumulation of the errors of LJ, charge, and polarization simulations. As it has been mentioned, relative free energy errors in the LJ and discharge simulations are about 0.3 and 0.4 kcal/mol, respectively. The error in the polarization simulations is estimated to be 0.3 kcal/mol for this model. This value has been obtained through the average difference between the two free energy values computed for each conformation. In contrast to LJ simulations, hysteresis values for the POL2 model are very small, 0.08 kcal/mol, with respect to the average difference of free energies (0.5 kcal/mol). The stdev obtained by the batch means procedure is only 0.03 kcal/mol. As these errors are smaller, hysteresis values and the batch means procedure are not suitable to give a good approximation to the error in the polarization simulations. For comparison, the same free energy error has been employed in all models, although DC and POL1 models may have slightly bigger error intervals because each polarization simulation has been performed only one time.

Additional series of free energy perturbations calculating the E^{Q} electric field in the same way as POL2 model but considering the inductive effect of induced dipoles among all sites of chorismate molecule (instead of only those separated by more than three bonds) were performed. In these FEP simulations, the polarization catastrophe appears when the atomic polarizabilities reach approximately to the half of their final values.

In the POL3 model, no interaction between polarization sites of the solute is considered. The E^{Q} electric field on the polarization sites of the chorismate is calculated as a function of the charges of the TIP4P waters as in the previous model. The inductive effect between dipole moments on the chorismate molecule is not considered now. So, with this model, the polarization is calculated without the iterative procedure. Table 2 shows the polarization free energy values, $\Delta G_{\mathrm{TIP4P}}^{\mathrm{POL3}}$, obtained for each conformation with the POL3 model. Each free energy value corresponds to the average of two FEP simulations. It can be seen that the diaxial conformations are more stabilized than the diequatorial conformations as in the previous model. The absolute free energies of polarization are also similar to the values obtained with the POL2 model. However, for every conformation, the $\Delta G_{\mathrm{TIP4P}}^{\mathrm{POL2}}$ value is more stable than its corresponding $\Delta G_{\mathrm{TIP4P}}^{\mathrm{POL3}}$ free energy. This fact is a consequence of the extra stabilization produced by the intramolecular inductive effect between induced dipole moments.

The stabilization of the AX3 conformation with respect to the diequatorial conformations because of the polarization free energy is about 2 kcal/mol. A significant proportion, 5%, for the AX3 conformation is obtained. However, this model yields less proportion for the diaxial conformations than the POL2 model and the experimental data. Errors for the POL3 model are obtained from the average of the differences between the two free energy values of each conformation. The calculated error is 0.35 kcal/mol, slightly greater than that obtained in the

POL2 model. The mean hysteresis value is 0.05 kcal/mol, and the stdev obtained with the batch means procedure is only 0.03 kcal/mol. Thus, as in the previous model, hysteresis and the batch means procedure are bad indicators of the error.

As an overall view, it should be noted that in the four models the relative polarization free energies of all of the conformations (Table 2) fall in a short interval of 2−4 kcal/mol. However, the clear separation between the values of the most significant diaxial conformation (AX3) and the diequatorial forms and the small error of each individual value (0.3−0.35 kcal/mol) makes clear the conclusion about each model: DC and POL1 increase the stabilization of the diequatorial conformations, whereas POL2 and POL3, in accordance with the experimental information, increase the stabilization of the diaxial conformations. When the relative polarization free energies are added to the LJ, electrostatic, and gas-phase contributions, the total relative free energies fall in a wider range of 10−13 kcal/mol. Despite that, the clear stabilization of the diaxial forms in the POL2 and POL3 models reduces the total free energy differences between the diaxial AX3 and AX5 forms and the diequatorial ones and produces a noticeable increase of the population of these diaxial conformations (Table 5). It should be noted the considerable error of the observed populations which is due to the sensitivity of the population values to energy variations and that the error of the total free energy values is 0.6 kcal/mol.

4. Conclusions

The conformational equilibrium of the chorismate molecule in water has been studied by means of FEP simulations. The decomposition of the calculation of the relative free energies of solvation in LJ transformations among geometrical structures and discharge and polarization processes for each conformation has been an efficient procedure to obtain precise results and to evaluate the importance of each energetic term in the conformational proportions.

The inclusion of solute polarization as is done in the POL2 and POL3 models is crucial to obtain diequatorial−diaxial conformational proportions compatible with the experimental values. In these two models, the solvent is described with a nonpolarizable TIP4P model and the solute polarization is modeled with atomic polarizabilities. It has been found that the best polarization energies are obtained when the charges of the chorismate dianion are not considered in the polarization of its own polarizable sites.

Another important factor to obtain a good description of the conformational equilibrium has been the consideration of all chorismate minima obtained in a previous exhaustive conformational search.[13] Previous FEP simulations of chorismate in water[12,14] could not reproduce the experimental conformational equilibrium because the study was done with few conformational minima and only the LJ and electrostatic terms in the intermolecular potential were considered.

On the other hand, the inclusion of a polarization center in the water molecules does not introduce a significant effect in the relative free energies of polarization of chorismate conformations. Solute polarization seems to be independent of considering explicitly the polarization in the solvent molecules (DC model) or in an average way (TIP4P model).

The conformational populations obtained in the present simulations and in a previous conformational study of chorismate with a PCM continuum model for water[13] are not coincident. The best FEP simulations yield similar proportions for the two diequatorial conformations; however, in the continuum solvent model, proportion intervals of 81−94% for EQ1 and 1−3% for EQ2 are obtained. In addition, the more stable diaxial conformation is not the same in both calculations: the AX5pcm conformation for the PCM calculations and the AX3 conformation in the present FEP simulations.

The hydrogen bond analysis performed with chorismate conformations shows that the diequatorial conformations have the smallest number of hydrogen bonds as can be expected from the formation of the internal hydrogen bond. However, relative free energy differences among diaxial conformations are not directly related to the total number of H bonds, because water molecules near the solute but not H-bonded to the chorismate have important stabilization effect. Also, energetic differences among H bonds of different solute functional groups are also significant.

Differences between free energies of solvation of two minima are mainly caused by differences in the geometrical structures. The contribution of the variation of atom charges among conformations is less important, but it has to be considered. A simple force field with the same charges for all chorismate conformations would lead to bad conformational results.

Some computational details of FEP simulations are crucial to obtain converged free energies. The system has to be equilibrated before the average stage of each window. It has been found that more configurations are needed to reach the equilibrium in the geometrical transformations than in the FEP simulations of discharge or polarization processes. Another important aspect is to sample a sufficient number of configurations to obtain converged average values. It can be suspected that the number of configurations is insufficient when the stdev calculated by the batch means procedure is clearly smaller than the obtained hysteresis values. This problem can be solved by enlarging the simulations for each window or averaging the results of different FEP simulations started at different initial molecular dispositions. Repetitions of FEP simulations have been performed to obtain an estimated error of 0.4−0.3 kcal/mol for the free energies of each perturbation process. More computational effort is needed to obtain converged results in the geometrical solute transformations. Finally, the influence of the selection of the perturbation path on the convergence is also very significant. Statistical important configurations of the perturbed systems have to be accessible from the configurations of the reference system. In the geometrical transformations of the solute, it has been found that the free energy errors are correlated with the geometric differences between two conformations.

Acknowledgment. Financial support from the Spanish Ministerio de Ciencia y Tecnología (Project BQU2000-0642-CO3-03) and from the Comissionat per a Universitats i Recerca de la Generalitat de Catalunya (2001SGR00301) are acknowledged. The Centre de Supercomputació de Catalunya C[4]-CESCA is also acknowledged for providing us with computer capabilities. S.M. benefited from a grant from Universitat de Barcelona.

References and Notes

(1) Haslam, E. *Shikimic Acid: Metabolism and Metabolites*; Wiley: Chichester, U.K., 1993.

(2) Weiss, U.; Edwards, J. M. *The Biosynthesis of Aromatic Amino Compounds*; Wiley: New York, 1980.

(3) Kast, P.; Tewari, Y. B.; Wiest, O.; Hilvert, D.; Houk, K. N.; Goldberg, R. N. *J. Phys. Chem. B* **1997**, *101*, 10976.

(4) Copley, S. D.; Knowles, J. R. *J. Am. Chem. Soc.* **1987**, *109*, 5008.

(5) Martí, S.; Andrés, J.; Moliner, V.; Silla, E.; Tuñón, I.; Bertrán, J. *J. Phys. Chem. B* **2000**, *104*, 11308.

(6) Martí, S.; Andrés, J.; Moliner, V.; Silla, E.; Tuñón, I.; Bertrán, J. *Theor. Chem. Acc.* **2001**, *105*, 207.
(7) Martí, S.; Andrés, J.; Moliner, V.; Silla, E.; Tuñón, I.; Bertrán, J.; Field, J. M. *J. Am. Chem. Soc.* **2001**, *123*, 1709.
(8) Kangas, E.; Tidor, B. *J. Phys. Chem. B* **2001**, *105*, 880.
(9) Worthington, S. E.; Roitberg, A. E.; Krauss, M. *J. Phys. Chem. B* **2001**, *105*, 7087.
(10) Wiest, O.; Houk, K. N. *J. Org. Chem.* **1994**, *59*, 7582.
(11) Wiest, O.; Houk, K. N. *J. Am. Chem. Soc.* **1995**, *117*, 11628.
(12) Davidson, M. M.; Guest, J. M.; Craw, J. S.; Hillier, I. H.; Vicent, M. A. *J. Chem. Soc., Perkin Trans. 2* **1997**, 1395.
(13) Madurga, S.; Vilaseca, E. *Phys. Chem. Chem. Phys.* **2001**, *3*, 3548.
(14) Carlson, H. A.; Jorgensen, W. L. *J. Am. Chem. Soc.* **1996**, *118*, 8475.
(15) Madurga, S.; Paniagua, J. C.; Vilaseca, E. *Chem. Phys.* **2000**, *255*, 123.
(16) Owicki, J. C.; Scheraga, H. A. *Chem. Phys. Lett.* **1977**, *47*, 600.
(17) Owicki, J. C. *ACS Symp. Ser.* **1978**, *86*, 159.
(18) Allen, M. P.; Tildesley, D. J. *Computer Simulation of Liquids*; Oxford University Press: Oxford, 1987.
(19) Jorgensen, W. L.; Madura, J. D. *Mol. Phys.* **1985**, *56*, 1381.
(20) Dang, L. X.; Chang, T. M. *J. Chem. Phys.* **1997**, *106*, 8149.
(21) Jorgensen, W. L.; Tirado-Rives, J. *J. Am. Chem. Soc.* **1988**, *110*, 1657.
(22) Jorgensen, W. L.; Severance, D. L. *J. Am. Chem. Soc.* **1990**, *112*, 4768.
(23) Kaminski, G.; Duffy, E. M.; Matsui, T.; Jorgensen, W. L. *J. Phys. Chem.* **1994**, *98*, 13077.
(24) Breneman, C. M.; Wiberg, K. B. *J. Comput. Chem.* **1990**, *11*, 361.
(25) Frisch, M. J.; Trucks, G. W.; Schlegel, H. B.; Scuseria, G. E.; Robb, M. A.; Cheeseman, J. R.; Zakrzewski, V. G.; Montgomery, J. A., Jr.; Stratmann, R. E.; Burant, J. C.; Dapprich, S.; Millam, J. M.; Daniels, A. D.; Kudin, K. N.; Strain, M. C.; Farkas, O.; Tomasi, J.; Barone, V.; Cossi, M.; Cammi, R.; Mennucci, B.; Pomelli, C.; Adamo, C.; Clifford, S.; Ochterski, J.; Petersson, G. A.; Ayala, P. Y.; Cui, Q.; Morokuma, K.; Malick, D. K.; Rabuck, A. D.; Raghavachari, K.; Foresman, J. B.; Cioslowski, J.; Ortiz, J. V.; Stefanov, B. B.; Liu, G.; Liashenko, A.; Piskorz, P.; Komaromi, I.; Gomperts, R.; Martin, R. L.; Fox, D. J.; Keith, T.; Al-Laham, M. A.; Peng, C. Y.; Nanayakkara, A.; Gonzalez, C.; Challacombe, M.; Gill, P. M. W.; Johnson, B. G.; Chen, W.; Wong, M. W.; Andres, J. L.; Head-Gordon, M.; Replogle, E. S.; Pople, J. A. *Gaussian 98*, revision A.5; Gaussian, Inc.: Pittsburgh, PA, 1998.
(26) Applequist, J.; Carl, J. R.; Fung, K.-K. *J. Am. Chem. Soc.* **1972**, *94*, 2952.
(27) Applequist, J. *J. Phys. Chem.* **1993**, *97*, 6016.
(28) Caldwell, J. W.; Kollman, P. A. *J. Phys. Chem.* **1995**, *99*, 6208.
(29) Meng, E. C.; Caldwell, J. W.; Kollman, P. A. *J. Phys. Chem.* **1996**, *100*, 2367.